

Article

First Attempt to Study Sedimentological Characteristics and Contamination Levels of Bottom Sediments in the Faanu Mudugau Blue Hole (Ari Atoll, Maldives)

Laura Cutroneo , Sarah Vercelli, Monica Montefalcone  and Marco Capello 

Department of Earth, Environmental and Life Sciences, University of Genoa, 26 Corso Europa, I-16132 Genoa, Italy; sarah.vercelli@edu.unige.it (S.V.); monica.montefalcone@unige.it (M.M.); marco.capello@unige.it (M.C.)

* Correspondence: laura.cutroneo@edu.unige.it

Abstract: Environmental contamination is ubiquitous and even in the ocean, signs of contamination of different types (chemical, biological, or plastic) are detected in all kinds of environments. In this study, a sediment core was sampled at the bottom of the Blue Hole of the Maldives (Ari Atoll) to make a first characterization of the sediment in terms of its grain size and organic–inorganic matter composition and to assess the sediment contamination levels in terms of trace elements (by ICP-MS analysis) and the eventual presence of microplastics (by optical classification and microRaman analysis of items). High concentrations of Hg (a maximum value of 0.145 ppm at the bottom layer of the core), Cd (a maximum value of 0.65 ppm at the core surface layer), and As (9.4 ppm at the top of the core) were highlighted at different layers of the sediment core. Plastic polymers were not detected in the sediment core, but 51 fibers characterized by the presence of artificial dyes or additives were found in the core (a mean of 5.7 fibers for each slice). The results confirmed the sediment contamination of the Maldivian Blue Hole, supporting the hypothesis of contamination due to ineffective waste management within the archipelago and mass tourism affecting the atolls.

Keywords: artificial fibers; trace elements; sediment core; blue hole; Maldives



Academic Editor: Wei Zhang

Received: 17 December 2024

Revised: 11 March 2025

Accepted: 24 March 2025

Published: 25 March 2025

Citation: Cutroneo, L.; Vercelli, S.; Montefalcone, M.; Capello, M. First Attempt to Study Sedimentological Characteristics and Contamination Levels of Bottom Sediments in the Faanu Mudugau Blue Hole (Ari Atoll, Maldives). *Environments* **2025**, *12*, 100. <https://doi.org/10.3390/environments12040100>

Copyright: © 2025 by the authors. Licensee MDPI, Basel, Switzerland. This article is an open access article distributed under the terms and conditions of the Creative Commons Attribution (CC BY) license (<https://creativecommons.org/licenses/by/4.0/>).

1. Introduction

Environmental contamination produced by anthropogenic activities is known to be widespread in all terrestrial, aerial, and marine environments [1,2]. Contamination is caused by the introduction of various substances and materials into the environment, including, among others, metals, hydrocarbons, pesticides, pharmaceuticals, and solid waste [3–6]. Some forms of contamination have a long history and have therefore been studied for years, such as metal-related contamination [7]; others have only been the subject of research for a few years (e.g., emerging contaminants) [8,9]. In the ocean, traces of contamination are found in all matrices: the surface layer and water column [10–12], sediments [13,14], and biota [15–17].

Regarding contamination by solid materials, the problem of plastic debris and microplastics (1 μm –5 mm plastic debris, MPs) is now one of the main objects of environmental studies. In fact, MPs constitute a universally recognized environmental problem, and it is known that they are present from the poles to the equator and in all environments (aerial, terrestrial, and marine) [18–20]. In the marine environment, their presence has been demonstrated at all depths in the water column [21–23], in sediments from shallow coastal areas [24,25] to abyssal and hadal areas [26–28], and in biota (fish, reptiles, mammals, and benthic organisms) [29–34].

Contamination is therefore also present in remote regions (such as Antarctica and the Arctic [35–37]), or regions considered “pristine environmental paradises” such as the archipelagos of tropical islands (the Seychelles, French Polynesia, the Bahamas, and the Maldives). In fact, these islands are not pristine [38,39] because they have towns and cities and commercial and industrial activities, and they are impacted by millions of visitors every year with consequent effects on the environment. In the case of the Archipelago of the Maldives, 1.88 million tourists from all over the world visited the atolls in 2023, occupying hotels, resorts, or vessels spread throughout the entire archipelago [40]. The influx of such a high number of visitors each year causes considerable management (supply of goods) and environmental impact (dispersion of solid waste and chemicals) problems, which puts the Maldivian Government under great pressure to study long-term precautionary and mitigation measures and strategies [41,42]. In fact, waste management strategies in the Maldives are mainly based on landfilling (Thilafushi Island) and open-air burning, and there are no wastewater treatment options [43–45].

Various research teams have confirmed chemical contamination in different matrices in the Maldives. For example, high concentrations of metals (Zn, Cu, Al, Cr, Sn, Pb, U, and V) were detected in coral skeletons in the North Male and South Male Atolls [46]. Persistent organic pollutants (POPs), such as polychlorinated dibenzo-p-dioxin (PCDD), polychlorinated dibenzofuran (PCDF), and dioxin-like polychlorinated biphenyl (DL-PCB), were found in soils related to the open burning of waste on islands [47]. Emerging contaminants (caffeine, fluoxetine, and norfluoxetine) were detected in reef sponges in the proximity of landfills [48]. Toxic heavy metals (Al, Cu, As, Cr, Mn, Ni, and Cd) were present in tuna fishes caught in the Laccadive Sea (North Maldives) [49]. Finally, heavy metals (Cu, Zn, and Fe) were recently found in seawater around Thilafushi Island, an artificial island created by the Maldivian Government in 1991 as a municipal landfill [50]. No data were found on the metal contamination status of marine sediments in the Maldives.

The presence of plastic and MPs has also been studied and confirmed in the Maldives’ islands. Imhoff et al. [51] assessed the abundance of plastic debris on shores and in natural accumulation zones in Vavvaru Island (Lhaviyani Atoll, North Maldives). They found a considerable amount of plastic debris (more than 1000 plastic particles per m^{-2}) in remote locations that are affected by ocean plastic transport. In the same atoll, Patti et al. [52] confirmed MP presence in sediments (more than 200 particles per kg^{-1} of sediment) across the fore reef, reef flat, and beaches on the small-inhabited Naifaruru Island. Saliu et al. [53] found plastic and charred MPs in sea surface water (0.32 ± 0.15 particles m^{-3}) and beach sediments (22.8 ± 10.5 particles m^{-2}) inside and outside the reef rim in the Faafu Atoll (central Maldives) even though the site is sparsely populated and not very touristy. In Magoodhoo Island (Faafu Atoll), Raguso et al. [54] established that 58% of the surveyed coral individuals (n. 38 individuals) were affected by the presence of MPs.

From the results of these previous studies carried out at different locations in the Maldivian archipelago and the lack of data on trace element contamination in Maldivian bottom sediments, we decided to perform one of the first exploration studies on the bottom sediments of the Blue Hole of Ari Atoll. The aim of the study was to make the first physical characterization of the sediment and the first assessment of the presence of contamination in terms of trace elements and MPs. Sampling took place in May 2022 as part of a scientific campaign that included the first physical–chemical characterization of the blue hole water column by measurements with a multiparameter probe [55]. Here, we present the results of the analysis carried out on the sediment core.

Blue Holes and Maldivian Blue Hole

Blue holes are submarine karst cavities with very peculiar chemical characteristics of their water masses (marked halocline, high concentrations of H₂S, and a marked deficit or total absence of oxygen), populated only by communities resistant to extreme environments, such as unicellular algae, bacteria, archaea, fungi, and foraminifera [56–58]. They are unique environments with very high scientific significance [57] that are found in various parts of the world and not easily accessible due to their morphology and depths. Among the best known in the world, the maximum depths of blue holes vary widely: 60 m for the Middle Caicos Island in the Bahamian Archipelago [59], 125 m for the Great Blue Hole of Belize [60], and 301 m for the Sansha Yongle Blue Hole in China, the world’s deepest marine blue hole [61]. A blue hole was also recently (in 2001) discovered in the Maldives archipelago (Figure 1), which is, so far, the only one discovered in the Indian Ocean. The Maldivian Blue Hole is in the Faanu Mudugau Lagoon in Ari Atoll [55,62] in the western part of the archipelago, and overlooks the Inner Sea, which cuts the archipelago longitudinally.

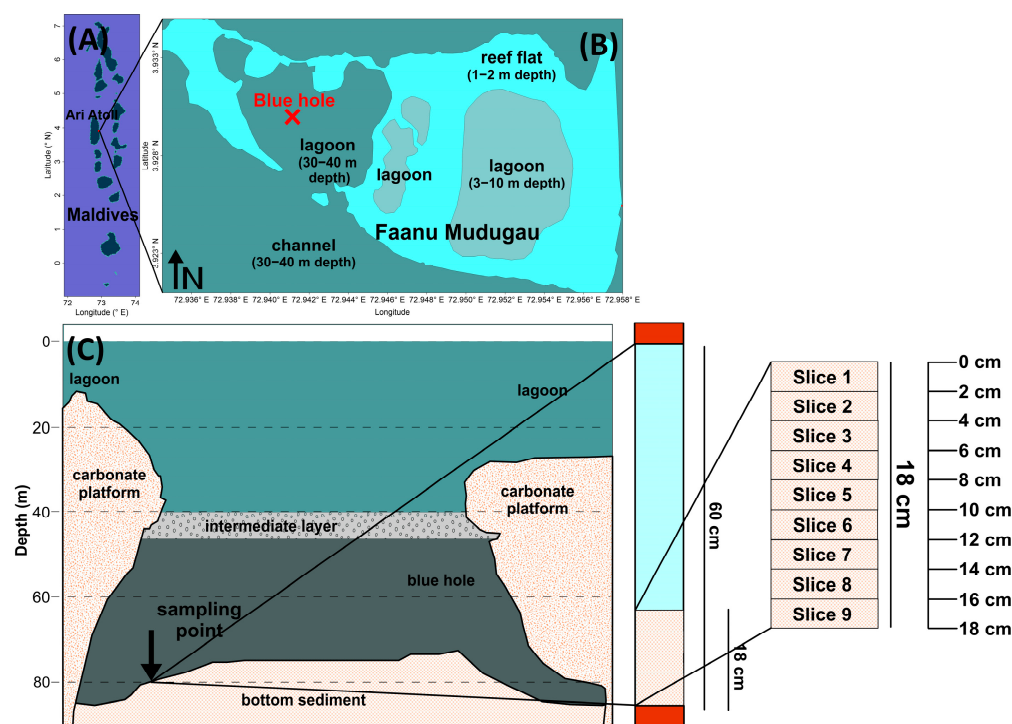


Figure 1. (A) A map of the archipelago of the Maldives and Ari Atoll; (B) the location of the blue hole (red X) inside the Faanu Mudugau Lagoon; and (C) a scheme of the vertical profile of the blue hole with the sampling point and the sediment core, with the subdivision in nine 2 cm slices.

Some blue holes are close to the coast and are easily accessible; therefore, they are highly frequented by tourists and are under increasing pressure from tourists practicing scuba diving or snorkeling. For example, the Egyptian Blue Hole was visited by more than 1000 visitors during the peak days in 2014 [63] with direct consequences on the surrounding coral reef and pollution of the marine environment. On the other hand, other blue holes are not the object of tourist visits and are almost undisturbed environments, except for the scientific activities that are carried out there. This is partly because of their inaccessible location and partly because they are poor in attractive marine populations on the walls and bottom (neither corals nor fish live in blue holes). This is the case of the Maldivian Blue Hole, which is an environment that is almost undisturbed by human presence. In fact, it is not a tourist site, and the nearest resort is 4.5 km to the NW and the nearest inhabited island

is 9 km away to the S. For these reasons, it is ideal for scientific research in oceanographic, geological, chemical, and biological features.

Because of their shape and lack of dynamics, blue holes are terminal collection sites for anything that settles from the water column and falls from the nearby coral reef lagoon [64]. Therefore, they are collectors of sediment, fecal pellets, dead organisms, coral fragments, and any extraneous object, such as MPs, carried by currents and introduced from the external environment (fibers or small particles carried by the wind). Bottom sediments of blue holes can thus be archives of climate variations and environmental contamination rates of the areas in which they are located [65]. For this reason, we decided to sample a sediment core from the bottom of the Maldivian Blue Hole and characterize the sediment (the grain size and organic–inorganic matter composition), investigating its level of contamination in term of trace elements and MPs.

2. Materials and Methods

2.1. Sampling

During the XXV Scientific Expedition organized by the University of Genoa (Italy), the International School for Scientific Diving, and the Albatros Top Boat (12 May 2022), SCUBA divers collected a shallow sediment core at 82 m of depth on the bottom of the Blue Hole of Faanu Mudugau (Ari Atoll, Maldives, 3°55.799' E 72°56.469' N; Figure 1).

Since this was the first time that sediment sampling was carried out within the Maldivian Blue Hole and therefore no past data on its composition and contamination were available, we decided to sample only one core to obtain the first baseline results. The choice to take a sediment core was made to obtain initial information on the vertical composition of the surface sediment of the blue hole bottom.

The choice of sampling method was determined by both our desire to alter and disturb the blue hole environment as little as possible and the need to visually inspect the sampling site before inserting the core liner into the bottom, so as to be sure of successful sampling. Therefore, sampling was carried out manually by very gently inserting a 60 cm long and 6 cm wide transparent Poly(methyl methacrylate) (PMMA) tube into the bottom sediment, avoiding disturbance of the sediment surface. Then, the tube was extracted from the bottom and closed with red rubber corks. This sampling method is often used for the extraction of short sediment cores, permitted us to choose the best sampling point, and allows for the steady and controlled insertion and extraction of the core tube [66–68]. The extraction of the core from the blue hole bottom was successful, but during the long ascension to the surface, the material inside the tube deposited on its base, producing a core with a final thickness of 18 cm.

Once on board, the sediment core was measured, photographed, and immediately sub-sampled into 9 slices 2 cm high using a steel paddle and a steel ring. The slices were stored in glass jars previously rinsed with micro-filtered water and sealed with aluminum film. In the laboratory, each slice was divided into several portions for subsequent analysis: grain size distribution, chemical composition, content of organic and inorganic matter, and MP presence. Finally, a portion of each slice was used to characterize the foraminiferal community present in the blue hole sediment. Foraminifera results are reported in Giraldo-Gómez et al. [69]. No replicates of the analyses were made because only one core was sampled and because only a few grams of the sediment were available.

2.2. Sample Grain Size and Chemical Analysis

An average of 15 g of the sample was used to perform the particle size analysis of the sediment following Cutroneo et al. [70]: samples were wet-sieved to divide the coarse fraction (diameter $\varnothing > 63 \mu\text{m}$) from the fine fraction ($\varnothing < 63 \mu\text{m}$). Then, the coarse fraction was dried and dry-sieved with a set of stainless steel sieves ($\varnothing < 63 \mu\text{m}$, $63 \leq \varnothing < 125 \mu\text{m}$,

$125 \leq \emptyset < 250 \mu\text{m}$, $250 \leq \emptyset < 500 \mu\text{m}$, $500 \leq \emptyset < 1000 \mu\text{m}$, $1000 \leq \emptyset < 2000 \mu\text{m}$, and $\emptyset \geq 2000 \mu\text{m}$), while the fine fraction was analyzed using a MultisizerTM 3 Coulter Counter (Beckman Coulter, Inc., Indianapolis, Indiana, USA).

The organic and inorganic sediment composition was determined by sediment combustion in an ISCO muffle (ISM320 mod.) at 550 °C for 3 h: the organic fraction was removed by combustion and the un-combusted (inorganic) fraction was determined by the weight difference from the total sample weight [71].

The sediment samples (0.5 g portion, previously pulverized) were also analyzed by inductively coupled plasma mass spectrometry (ICP-MS) after modified aqua regia digestion (1:1:1 HNO₃:HCl:H₂O). The concentration of 53 elements was determined, including those considered most significant as indicators of anthropogenic contamination (Ca, Fe, Mg, Mn, As, Cd, Co, Cr, Cu, Ni, Pb, V, Zn, and Hg). Procedures to ensure the quality of the results included analysis of blanks; a test on the certified reference material standards; and duplicate samples to ensure reproducible results [72]. Analysis was performed by the Bureau Veritas Mineral Laboratories of Vancouver, Canada (ISO 9001 Quality Management Systems).

2.3. Sample Treatment, Analysis, and Precautions for Microplastic Research

A 50 mL portion of the sample was used to search for MPs in the blue hole sediment.

The sediment samples were placed in Pyrex beakers, dried in a thermostatic oven at 60 °C, and weighed (average weight of 20 g). Then, 200 mL of super-salted pre-filtered water with a density of 1.3 g cm⁻³ was added to each sample. The super-salted water was obtained by adding 2.4 kg of MgCl₂ to 1 L of fresh water. MgCl₂ was chosen because it is neither toxic nor harmful and because it allows for a higher-density solution than that obtained using NaCl [73]. The mixtures of the sediment and super-salted water were stirred for 2 min with a glass rod and allowed to settle for 48 h. The supernatant was collected with a pipette and poured into a glass jar. The operation was repeated three times until 30 mL of the supernatant for each sample were obtained.

Ten mL of 4% HCl was added to the supernatant for the removal of the abundant carbonaceous particles present. Due to the carbonate nature of the sediment, the abundant presence of foraminifera in the samples, and the low presence of organic matter, HCl was used to treat the samples in place of the commonly used H₂O₂, following the results of the study conducted by Pfeiffer and Fischer [74]. In fact, they showed that, in the case of a calcareous matrix, HCl can be used for digestion at a maximum concentration of 10% and at a reaction temperature of 20 °C because it effectively consumes the calcareous material and shows no distinct effect on any of the synthetic polymers [74]. HCl was left to act for 96 h at room temperature (18–20 °C).

Afterward, the supernatants were filtered through GF/F glass microfiber filters (diameter 47 mm, pore 0.7 μm; WhatmanTM, GE HealthCare UK Limited, Little Chalfont, UK) and rinsed with 2 L of pre-filtered fresh water to remove salt residues and prevent crystal formation. Finally, the filters were placed in glass Petri dishes.

The identification (shape), counting (number), measurement (size), and classification (color) of the items collected on the filters were performed using an optical microscope Leica Z16 APO (5× magnification), managed by Leica Application Suite 3 (Leica Microsystems, Mannheim, Germany) analysis software [27].

Following [27,75], the items (at least 10% of the items characterized for each filter) were analyzed using a XploRATM PLUS MicroRaman spectrometer (Horiba Scientific, Ltd., Kyoto, Japan) with the LabSpec 6 Spectroscopy Suite software (Horiba Scientific, Ltd., Kyoto, Japan) of the Department of Earth, Environment, and Life Sciences of the University of Genoa. The choice to use μRaman spectroscopy was made because it is a widely and successfully employed method in the study of MPs dispersed in the environment, as is

Fourier-transform infrared (*F-TIR*) spectroscopy [76]. The identification of item materials was conducted by comparing the obtained spectra with the Spectral Library of the Wiley’s KnowItAll® Software (version 24.2.72.0; John Wiley & Sons, Inc., Hoboken, NJ, USA). Only results with correspondence of >70% to the reference spectra were accepted; spectra with a match of <70% were classified as “unrecognized”.

All the instrumentation used in the laboratory was rinsed previously with pre-filtered fresh water, the operators wore cotton coats, and the air exposure of the samples was reduced to the bare minimum to minimize the contamination of the samples. A control filter was placed next to the samples when they were exposed to air during laboratory operation and μ Raman analysis. All materials used in the sampling process (core tube and red rubber corks) and laboratory (paper filters, paper towel, and sample filters) were analyzed by μ Raman so that they could be identified and not considered if found in the samples.

The diagram in Figure 2 summarizes all of the steps that were carried out for the study of the presence of MPs in the Maldivian Blue Hole, placing emphasis on specific measures to be taken into consideration in the laboratory and during analyses. In detail, the black boxes show the different steps of sample treatment and item analysis; the red boxes show the precautions taken to minimize the contamination of samples during their handling and the checks that were carried out on the materials used for sampling, sample treatment, and analysis in laboratory; the blue boxes show the use of the control filters to detect and, if necessary, eliminate items due to any external contamination of the samples.

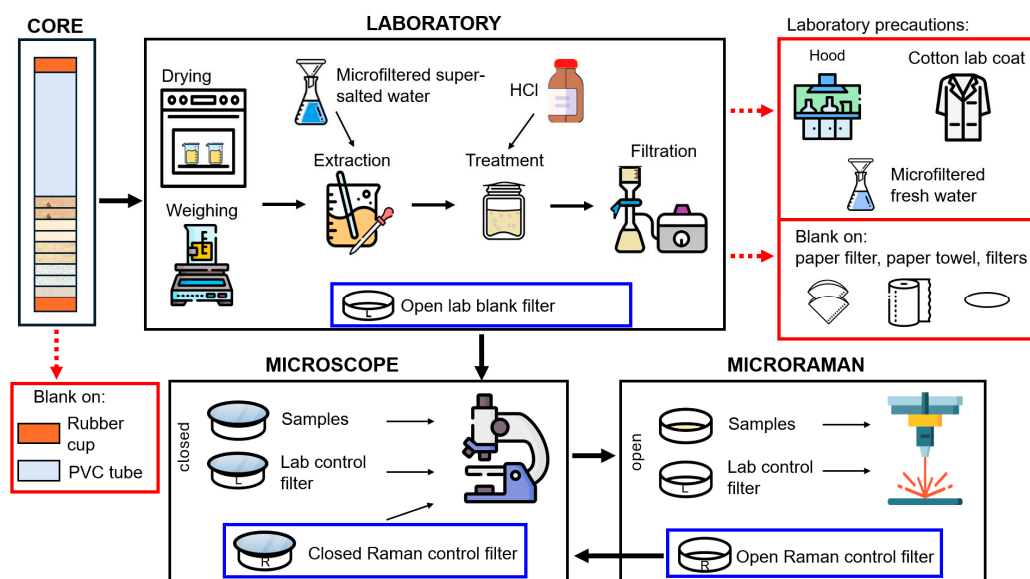


Figure 2. A schematic representation of all steps (in black), all materials and precautions (in red), and the control filters (in blue) used in the extraction and analysis of microplastics in the sediments of the Maldivian Blue Hole core.

In terms of precautions, it was essential to use control filters when the samples were exposed to air to be able to detect the presence of particles unrelated to the samples but due to the handling of them. The items found on the control filters underwent the same treatment as those of the samples and were then listed, photographed and analyzed with μ Raman. Subsequently, if these items were also present in the samples, they were removed from the count. This step in the procedure for the determination of MPs in environmental samples is essential to have greater confidence in the robustness of the results and thus in the assessment of the actual MP contamination of the environment under investigation. In fact, during treatment and analysis, samples are inevitably exposed to the air and, therefore, can be contaminated at any time by the environment in which they are exposed. In the

specific case of the Maldivian Blue Hole, it was possible to identify 29 items (55% fibers and 41% fragments) on the control filters.

Finally, it should be noted that blue (Copper phthalocyanine) fragments were found in the control filter (Figure 3). The discovery of these granules in the control filter made it clear that these fragments were already present in the virgin filters, leading to their automatic exclusion from the counts whenever they were detected in the samples. This situation emphasizes the importance of the “anti-contamination” precautions taken in the handling of samples and during analysis in order to avoid erroneously indicating the presence of MPs in the environment.

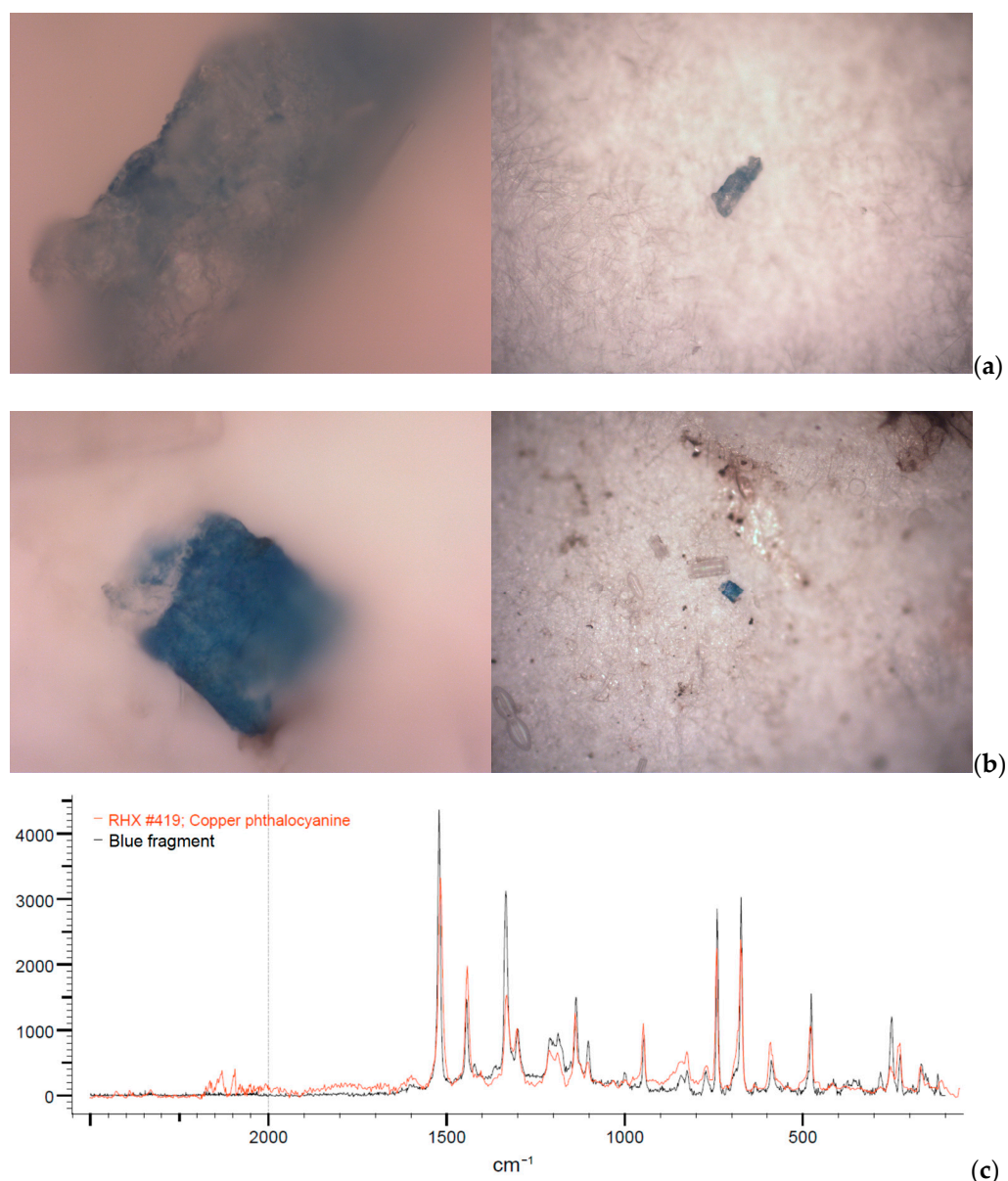


Figure 3. Images taken at μ Raman with 100 \times (left) and 10 \times (right) magnification of the blue fragments found in the control (a) and samples (b) filters; (c) the spectrum obtained by μ Raman analysis (in black) and the resulting spectrum in the reference spectra library (in red).

2.4. Assessment of Ecological Risks

The chemical concentrations of eight elements (As, Cd, Cu, Cr, Ni, Pb, Zn, and Cr) found in the blue hole core were used to assess the degree of contamination and the associated ecological risk of the core sediments. Two assessment indexes were considered: the Pollution Load Index (PLI) and Potential Ecological Risk Index (PERI), following [77].

2.4.1. Pollution Load Index (PLI)

The PLI is used for the total assessment of the degree of sediment contamination and comparison among the core slices. The PLI is calculated starting from the Contamination Factor (CF) values of each considered element with the following equation:

$$PLI = (CF_1 \cdot CF_2 \cdot CF_3 \cdot \dots \cdot CF_n)^{-n}, \tag{1}$$

where CF is the ratio of the concentration of each element in the sediment with the concentration of those elements in the background, and n is the number of considered elements ($n = 8$). Since background values were not available for the Maldives, the general upper continental crust (UCC) [77] values were considered. The UCC values are reported in Table 1.

Table 1. The upper continental crust (UCC) values (in ppm) and the toxic response factor (T_r) for the eight trace elements considered in the sediment core [77].

Trace Element	UCC	T_r
As	2.0	10
Cd	0.2	2
Cu	14.3	5
Cr	35	2
Ni	18.6	5
Pb	17	5
Zn	52	1
Hg	0.056	40

Sediments are considered as “polluted” if $PLI > 1$; sediments are “non-polluted” if $PLI < 1$. $PLI = 1$ is the baseline level of pollution.

2.4.2. Potential Ecological Risk Index (PERI)

The PERI is a well-known method for assessing the potential risk of trace element pollution in sediments, considering the total trace element concentration and the toxic response factors for each element [78].

$$PERI = \sum E_r, \tag{2}$$

where E_r is the ecological risk factor:

$$E_r = T_r \cdot CF, \tag{3}$$

where T_r is the toxic response factor. T_r has a standard value for each element [77]. T_r values for the eight trace elements considered in this study are reported in Table 1.

Considering E_r results, the ecological risk of the bottom sediments is classified as follows: “low” with $E_r < 40$; “moderate” with $40 \leq E_r < 80$; “considerable” with $80 \leq E_r < 160$; “high” with $160 \leq E_r < 320$; and “very high” with $E_r \geq 320$ [77].

Considering the PERI results, the potential ecological risk is “low” with $PERI < 90$, “moderate” with $90 \leq PERI < 190$, “considerable” with $190 \leq PERI < 380$, and “very high” with $PERI \geq 380$ [77].

2.5. Statistical Analysis

Principal Component analysis (PCA) was applied to the results of the physical characteristics of sediments and element concentrations found in core slices to identify the most characterizing parameters within the slices. PCA was conducted by R package “vegan” (version 3.5.3) [79].

3. Results and Discussion

3.1. Grain Size and Organic–Inorganic Content

The results of sediment size classification are summarized by the modified Shepard triangle diagram [80] of Figure 4. The first slice (0–2 cm) is characterized by the prevalence

(85%) of the grain size fraction < 63 μm (the fine fraction). Slice 2–4 cm is almost equally composed of fine fraction, sand, and gravel (43, 24, and 33%, respectively), with the maximum percentage of gravel among the slices. Slices 4–6, 6–8, and 8–10 cm show a gradual increase in sand, with a decrease in the fine fraction and an almost constant percentage of gravel. Quite the opposite, slices 10–12, 12–14, and 14–16 cm have a constant portion of sand, but show a progressive decrease in gravel with a consequent increase in the fine fraction. Sample 16–18 cm is mostly composed of fine fraction (55%), with 35% of sand and 10% of gravel. Sample 0–2 cm is mostly composed of fine fraction (85%), with 15% of sand and 0% of gravel.

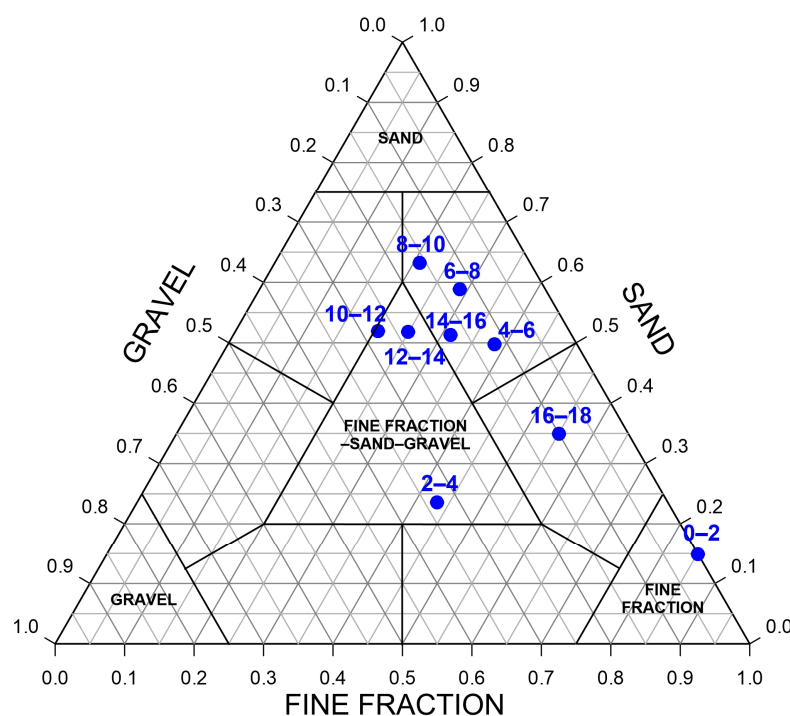


Figure 4. Modified Shepard's triangle diagram for sediment samples.

In 2006, in a study on surface sediment samples in Ari Atoll, Gischler [81] found that, generally, bottom sediments consist of only 0.7% of fine fraction (<125 μm), but that fine fraction preferentially accumulates in the deepest lagoon parts. They found that sediments were made up of aragonite (78%), high Mg-calcite (20%), and low Mg-calcite (2%). Morgan and Kench [82], studying the sediment fluxes in the North Male Atoll, defined that bottom sediments were typically sand size, in contrast to what was found in the blue hole core. Seasonal variations were highlighted in sediment transport by Morgan and Kench [82]: during the NE monsoon period, sediment transport was characterized by finer sediments (fine to medium sand), while during the SW monsoon period, sediment transport was characterized by medium sand and gravel. Analyzing the tidal flow regime and sediment transport in North Male Atoll, Rasheed et al. [83] assumed that the main mode of sediment transportation is the wind-driven transport for shallow lagoon areas of the Maldives archipelago, but that tides dominate the sediment transport regime in the shallow water areas. The Male area is affected by a relatively low mean spring tidal variation of 0.97 m but is characterized by strong diurnal and seasonal differences. In fact, high tides and low tides have different heights [84] which can therefore influence sedimentation in different ways.

The prevalence of the fine fraction in the uppermost layer of the blue hole core indicates the prevalence of fine sedimentation within the blue hole from the surrounding lagoon, confirming that, usually, the lagoon is characterized by calm dynamic conditions. The constant input of fine carbonate material (with varying concentrations of organic material dependent on the season) usually falls into the blue holes under fair weather conditions,

as evidenced by Gischler et al. [85] and Schmitt et al. [60]. The progressive increase in granule size in the underlying slices may be an indication of a high-energy event (e.g., strong seasonal monsoons, tsunamis, or flood events [84]) that resulted in coarser material settling in the Maldivian Blue Hole.

The dynamics within the atolls and lagoons are governed by tides and the surface currents [86] that flow through the channels between the lagoons and the openings in them. The combined currents, driven by tides and wind, can exceed speeds of 2 m s^{-1} [83]. General circulation in the region is governed by the monsoon regime. The monsoon climate of the Maldives governs local circulation and sedimentary deposition to such an extent that it conditions and forces the morphology of the atolls themselves [87]. The increase in the fine fraction in the last sections of the core would reflect the normal sedimentation of the area and thus the limit of the disturbance event represented by the central slices of the core. This is supported by the study carried out by Morgan and Kench [82] in the North Male Atoll: the authors used sediment traps to quantify the sedimentation rate on the reef platform under the different actions of the two monsoon regimes that characterize the Maldivian climate. Morgan and Kench [82] verified that 95% of transport occurs during the southwest monsoon period with rates of up to $1905 \text{ g m}^{-1} \text{ d}^{-1}$. This confirms that the component of sediment transport is very important in the coral reef environment and that processes involving sediment handling include the filling of lagoons with outer sediments [82].

Due to their proximity to the equator, the Maldives are generally not affected by storms; only the northern parts are occasionally affected by cyclones [81]. However, the archipelago is affected by large-scale events such as tsunamis or flood events [81,84]. For example, the Indian Ocean tsunami of 2004 had a devastating impact on the archipelago and its population as well as the two flood events (long wave period up to 20 s) of April 1987 and May 2007 [84]. The first flood event was generated by a storm propagating from the southern Indian Ocean with a wave period of 15–16 s and a significant wave height (H_s) of about 3 m in deep water and much larger near the coasts (a maximum wave height of 5 m in Male). The 2007 flood event was generated by two consecutive storms from the South Indian Ocean and South Africa; it was characterized by an 18–20 s wave period and a H_s peak of 3.05 m. Both events had devastating effects on the Maldivian islands [84] and may have played an important role in the sediment transport into the atolls and hence into the blue hole, bringing coarse material into it. However, we have no direct indication from our results that the increase in sediment size in the central section of the core was due to solid transport from these strong events.

Giraldo-Gómez et al. [69], in a parallel study on foraminiferal tests in the Maldivian Blue Hole core, found that sediment transport mostly occurs over very short distances, and all material was recently deposited on the bottom of the blue hole. This study suggests that the core is made up of recent material from nearby areas but does not provide any additional indication of sedimentation rates, the time corresponding to the 18 cm of the core, and the grain size vertical distribution.

Figure 5 summarizes the percentage composition of the slices in fine and coarse size fractions and organic–inorganic content. The organic fraction was between 3.4 and 4.5%. The trend of the organic–inorganic composition along the core mirrors the trend of the size class abundances: as the coarse portion of the sediment increases, the percentage of inorganic material in the samples increases; thus, it confirms that the organic fraction is more closely related to the fine fraction [88].

Consistent with the above grain size consideration, the higher concentrations of organic matter in the surface layer of the core can be explained by the fall in the blue hole of material from the lagoon. Once at the water/sediment interface on the bottom of the blue hole, the organic material can undergo the degradation process and can thus lead to a

gradual concentration decrease in the underlying layers of the core [89]. Its decrease in the intermediate layers of the core may also support the hypothesis of more dynamic events that did not allow the fine fraction and organic matter to settle. The return to the normal sedimentation regime in the bottom core layers is supported by the increase in the organic material not yet degraded.

The grain size partition in the core can be a testimony to the special depositional environment represented by blue holes [65].

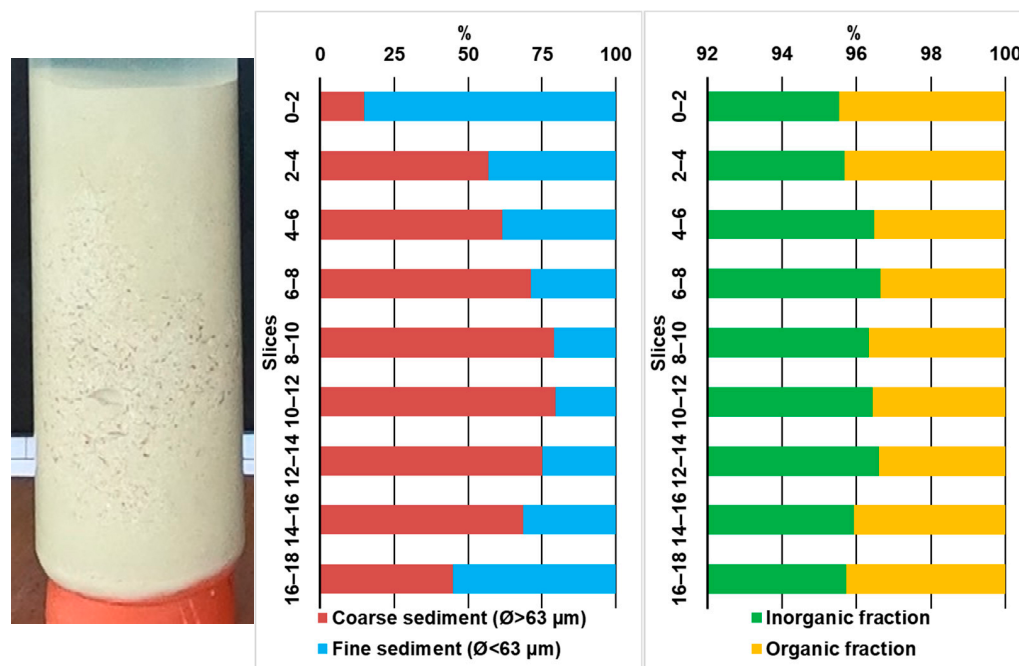


Figure 5. An image of the core (left) flanking the grain size distribution (center) and inorganic–organic fraction composition (right) of the sediment in the different slices (from 0–2 to 16–18) of the core sampled from the bottom of the Maldivian Blue Hole. The x-scale in the graph of the inorganic and organic fractions is displayed with a range of 93–100% to highlight the variation in the otherwise barely visible percentages of the organic fraction.

3.2. Major and Trace Elements

Calcium, the main constituent of the carbonate atoll sediments, shows concentrations ranging from a minimum of 24% of the third (4–6 cm) slice to a maximum of over 40% (not measured by the method of analysis used) of the first slice (0–2 cm). Mg, a major component of dolomite with Ca and frequent carbonate present in the Maldives [90], is between 0.7 and 1.1%. Strontium is >2000 ppm in all samples, confirming its close association with carbonate sediments including Maldivian sediments (high Sr aragonite-rich carbonate (HSAC) sediments), as shown by Alonso-Garcia et al. [91].

Ca, Mg, S, and P (Figure 6) have the same trend in the sediment core: the maximum in the first slice (0–2 cm), the minimum in the third (4–6 cm for Ca, P, and Mg) or second slice (2–4 cm for S), and an increase towards the bottom of the core. Iron shows values of 0.01% at most.

Among the trace elements (Figure 7), Cu, Pb, and Zn show decreasing values along the core, with the highest values in the third (4–6 cm for Cu and Pb) or second (2–4 cm, for Zn) slices. Cd and As have the highest concentrations (0.65 and 9.4 ppm, respectively) in the first slice (0–2 cm). In contrast, Cr and Hg show their maximum concentration at the bottom of the core (16–18 cm), with 6.0 ppm and 0.145 ppm, respectively. Ni, Cr, and Hg concentrations have a similar trend from the top to the bottom. In general, the first slice is found to have the highest contamination overall.

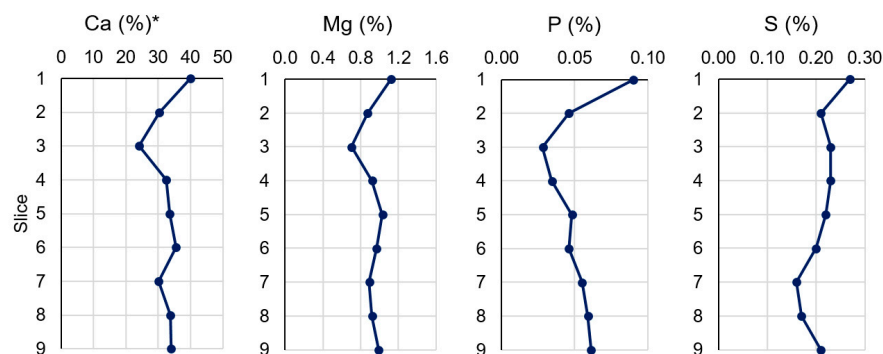


Figure 6. Major element concentrations (in %) in the 9 slices of the sediment core from the first on the top (1: 0–2 cm) to the last on the bottom (9: 16–18 cm). * the Ca concentration is >40% in the first slice.

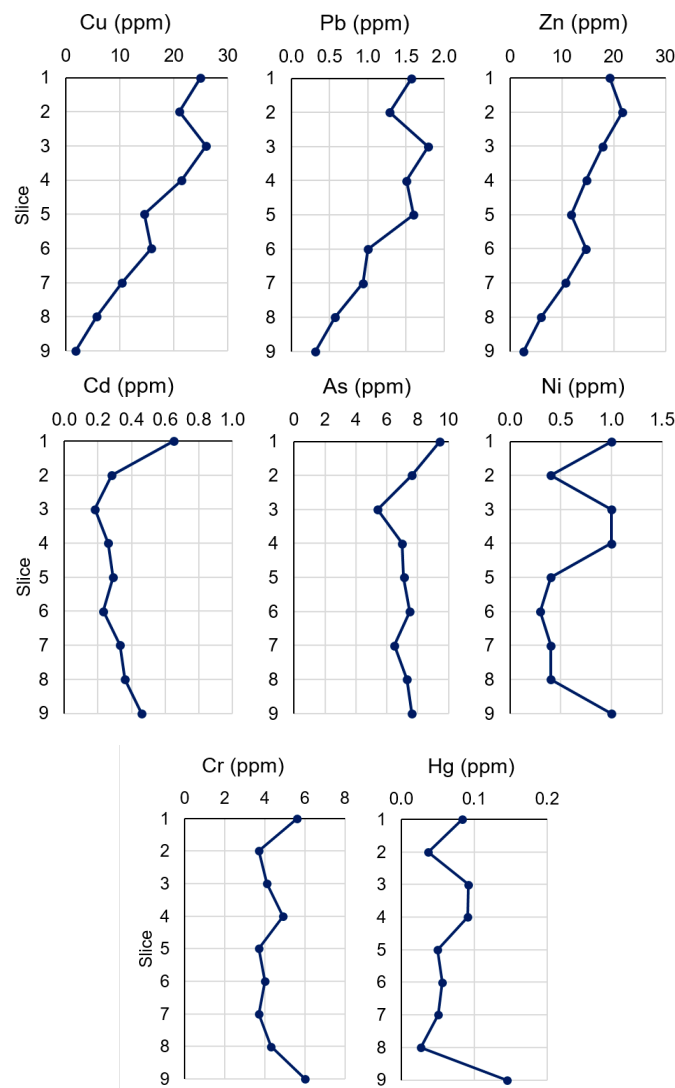


Figure 7. Trace element concentrations (in ppm) in the 9 slices of the sediment core from the first slice (top, 0–2 cm) to the last one (bottom, 16–18 cm).

Mercury concentration in marine sediments depends on the local lithologies but is often used as an indicator of anthropogenic contamination. In accordance with this, many governments have established environmental quality standards (EQSs) for Hg (as a priority substance) in sediments. For example, Italy (the Mediterranean Sea) has defined the EQS for Hg as 0.30 ppm following the European Commission strategic objectives [92], and Canada has established this

as 0.13 ppm following the Canadian Environmental Protection Act [93]. No EQSs are defined for the Maldives sediment. The maximum Hg concentration found in the bottom core slice is half of the Italian EQS, but twice the Canadian one, thus corresponding to an unexpectedly high value. A study was conducted in the framework of the Minamata Convention [94] in 2019 to identify the status and existing challenges to mercury management and regulation in the Maldivian archipelago. The Maldives does not produce objects or materials containing Hg and does not mine it, so all Hg present is imported from abroad. However, the archipelago is exposed to Hg contamination derived from its release in the environment produced by the practice of open-burning waste on islands and placing waste in open storage areas [94].

Following the standard guidelines of safety limits for metal concentrations in marine sediments (as defined by the United States Environmental Protection Agency (US EPA) and reported in [95]), the maximum value of As found in the Maldivian Blue hole (9.4 ppm) is indicative of a sediment defined as “polluted”. The maximum value of Cu (25.9 ppm) is at the lower limit of sediments classified as “moderate polluted”, while concentrations of Cr, Ni, Pb, and Zn correspond to a “non-polluted” sediment.

Cadmium concentrations found in the blue hole sediment ranged between 0.18 and 0.65 ppm. Following, for example, the Italian law limits for Cd concentration in marine sediments (0.3 ppm; Italian Ministerial Decree n. 260/2010 and Legislative Decree n. 172/2015) [92], concentrations found indicate that the first layer and the three deepest layers of the core have relatively high values. Worldwide, Cd-Ni batteries, landfills, use of agricultural fertilizers, vehicular emissions, and inappropriate waste disposal are the main sources of Cd pollution in the environment [96]. Mikhailenko et al. [97] highlight that Cd pollution has a direct relationship with tourism as a result of hotel wastewater and increased traffic. Therefore, all these aspects may contribute to the presence of Cd in the Maldivian sediments.

Arsenic pollution is derived from chemicals used in agriculture such as herbicides, fungicides, and insecticides [98]. Although agriculture is not an extensive activity on the Maldivian islands, pesticides and insecticides are regularly used at resorts to combat mosquitoes, bedbugs, and cockroaches or on golf courses to ensure the integrity of grass fields [99].

3.3. Pollution and Ecological Risk Assessment

The results of the pollution and ecological risk assessment are reported in Figure 8. All PLI results show “non-polluted” sediments, while the PERI highlights a “moderate” ecological risk in four slices (1, 3, 4, and 9). This last result is mainly influenced by the E_r of As and Hg; in fact, the E_r of As was “moderately high” in the first slice, and the E_r of Hg was “moderately high” in slices 1, 3, 4, and 6, and “considerable” in the bottom slice.

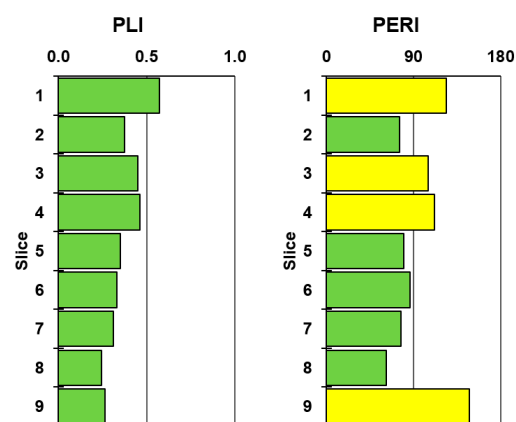


Figure 8. The Pollution Load Index (PLI) (left) and Potential Ecological Risk Index (PERI) (right) results for each core slice of the blue hole. In green are the results corresponding to “non-polluted” sediments (PLI < 1), and “low” potential ecological risk (PERI < 90); in yellow is the “moderate” ecological risk (90 < PERI < 190).

3.4. PCA Results

The PCA result (Figure 9) summarizes well the differences between the core slices and highlights the following three groupings of slices: slices 1 and 9 are completely separated from the others due to the prevalence of fine-size components and high values of elements such as Ni for slice 1, and Hg, Cd, and Cr for slice 9; slices 2, 3, and 4 are grouped together due to the high concentrations of Pb, Zn, and Cu; and samples 5–8 are separated from the others depending on their coarse component.

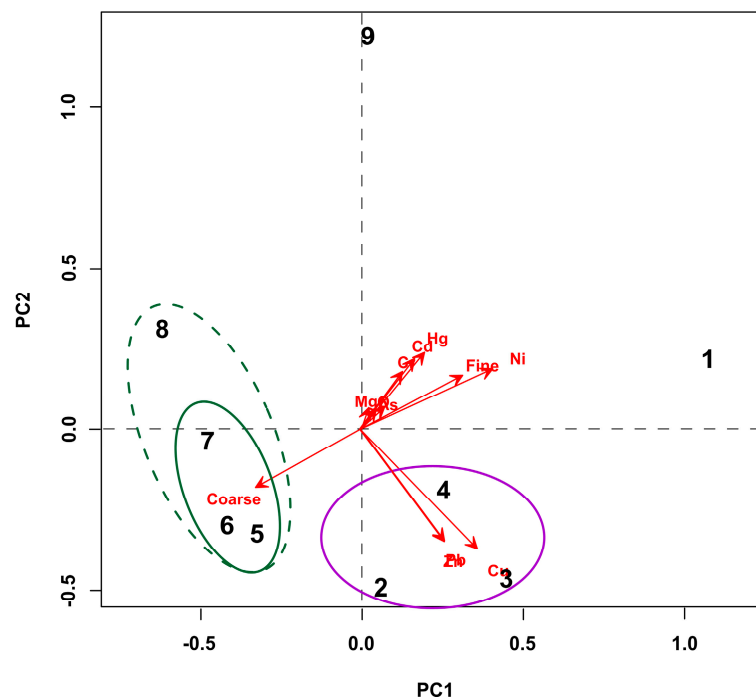


Figure 9. PCA results. The black numbers are the core slices; in red, elements, coarse, and fine components of the sediment, and inorganic (I) and organic (O) fractions. Superimposed, the purple and green circles grouping slices 2, 3 and 4, and 5–8, respectively. PC1 explains 43% of the variance; PC1 and PC2 explain 80% of the total data variation.

3.5. Items Results

The results of the characterization of items extracted from the core sediments are reported in Table 2. A total of 984 items were counted and classified: fragments (34%) and fibers (25%) are the most represented shape; brown (26%), black (20%), and blue (16%) are the most frequent color; and the items are sized mostly between fine fraction (<63 μm) and 500 μm (84%) reflecting grain size characteristics of the sediment. The first slice (0–2 cm) of the sediment core is the richest in items, followed by the lower layers.

Among items analyzed with μRaman , no plastic polymers were identified, but 51 fibers (a mean of 5.7 fibers for each core slice) characterized by the presence of artificial dyes or additives (such as carbon) were detected. Other materials identified with μRaman include chitin fibers, particles of Fe oxides, carbonates (remaining despite HCl digestion), SiO_2 , and one paracrystalline carbon particle.

The fiber composition was been defined, but only dyes or additives were, because one of the main problems with μRaman detection technology is the spectral distortion caused by the fluorescence signals. Fluorescence signals result from micro-biological, organic, or inorganic items [76] and some plastic additives (such as pigments), which lead to a low signal-to-noise ratio in the μRaman spectra of MPs [100,101].

Table 2. The results of the classification of items extracted from each slice of the sediment core of the Maldivian Blue Hole.

Slice	1	2	3	4	5	6	7	8	9
Number of items	207	93	72	79	123	62	57	153	138
Grain size classification (in %)									
Ø ≥ 2000 µm	0.0	1.1	1.4	5.1	1.6	1.6	5.3	0.6	0.0
1000 µm ≤ Ø < 2000 µm	1.4	5.4	8.3	6.3	4.1	8.1	10.5	3.3	7.3
500 µm ≤ Ø < 1000 µm	4.4	8.6	13.9	13.9	10.6	19.3	10.5	6.5	9.4
250 µm ≤ Ø < 500 µm	9.2	19.3	32.0	12.7	11.4	19.4	28.1	14.4	10.1
125 µm ≤ Ø < 250 µm	18.8	32.3	19.4	30.4	21.9	22.6	26.3	32.7	23.9
63 µm ≤ Ø < 125 µm	34.8	25.8	19.4	24.0	34.1	25.8	15.8	28.1	31.9
Ø < 63 µm	31.4	7.5	5.6	7.6	16.3	3.2	3.5	14.4	17.4
Shape classification (in %)									
Fibers	7.7	28.0	44.4	32.9	29.3	27.4	47.4	11.7	35.5
Fragments	34.3	24.7	27.8	34.2	33.3	41.9	22.8	39.9	39.1
Granules	1.0	12.9	11.1	6.3	4.9	9.7	26.3	19.6	5.1
Other	57.0	34.4	16.7	26.6	32.5	21.0	3.5	28.8	20.3
Color classification (in %)									
White-Cream	24.2	20.4	20.8	12.6	10.6	6.5	5.3	4.6	11.6
Orange	16.4	7.5	9.7	13.9	26.8	16.1	8.8	15.7	6.5
Blue	5.3	19.3	27.9	11.4	20.3	14.5	29.8	11.1	23.2
Black	17.9	19.4	19.4	25.3	9.0	27.4	26.3	27.5	15.2
Brown	28.5	28.0	12.5	20.3	24.4	27.4	15.8	34.6	27.5
Other	7.7	5.4	9.7	16.5	8.9	8.1	14.0	6.5	16.0
µRaman results (in %)									
Artificial dyes/additives	21	11	12	30	12	16	13	24	30
Other components	8	3	9	4	15	0	0	3	5
Not recognized	71	87	79	67	73	84	87	72	66

Two techniques are most used in the study of items dispersed in the environment, Raman and Fourier-transform infrared (F-TIR) spectroscopy [102,103]. Recent studies have compared the two techniques, highlighting the pros and cons of each: e.g., Raman is the most suitable for the identification of small ($5 < \text{Ø} < 500 \text{ }\mu\text{m}$) MPs, although it requires more time than F-TIR [103,104]; F-TIR does not have the disadvantage of fluorescence, but suffers interference with water [76]. The results of these comparisons confirm that both techniques are valid and that using them in a combined manner would be ideal for a more correct and complete characterization of MPs dispersed in the environment [76,102]. This ideal combination is counterbalanced by an important economic component for the purchase and/or use of the two instruments.

In the case of the Maldivian Blue Hole, although it was not possible to determine the material of the fibers, dyes/additives were detected, thus highlighting the anthropic nature of these items. In turn, the presence of synthetic-colored fibers, although not composed of plastic materials, highlights the problem of the release of fibers into the environment and their extreme persistence in the marine environment [105]. Numerous studies have addressed the different behavior of MPs in the ocean, highlighting differences in surface drifting, transport in the water column, and settling based on shape, density, degradation, fouling coverage, etc. [106]. Among the dispersed items, fibers have the lowest sedimentation velocity and can therefore remain in the water column longer and travel greater distances with currents [52]. Furthermore, fibers, even with dimensions greater than $1000 \text{ }\mu\text{m}$, can easily be transported in the air by wind and therefore can reach every part of the Earth’s surface, more easily than items of other shapes [107]. This may explain the absence of MPs in the shape of fragments or granules within the Maldivian Blue Hole sediments.

4. Conclusions

A sediment core sampled from the bottom of the Blue Hole in the Maldives (Ari Atoll) was analyzed to make an initial physical characterization of the sediment and an

assessment of the sediment contamination of trace elements and microplastics. Some evidence of contamination was found for trace elements such as Hg, As, Cd, and Cu. Artificially colored fibers were found in all slices of the core. These make the blue hole an interesting study site for determining the diffusion of pollutants in the Maldivian marine environment and an archive of the degree of environmental contamination around it. The peculiar distribution of sediment particle size classes found in the core highlights the need for future studies on sedimentation rates within the lagoon and the blue hole, and studies on the effect of seasonal and extreme events on sedimentation. Future studies on sedimentation rates and sediment dating could also help to understand the timing involved in sedimentation inside the blue hole. Moreover, the high values of trace elements found in the blue hole sediments draw attention to the spread of contamination in the Maldives archipelago. These findings, and the fact that other studies have found high values of trace elements in coral skeletons, tuna fishes, and seawater, indicate the need to further investigate the degree of contamination of the Maldivian marine environment and to carry out an archipelago-wide study of bottom sediment contamination, which is lacking to date.

Author Contributions: Conceptualization: M.C. and L.C.; Resources: M.C. and M.M.; Writing—original draft: L.C.; Writing—Review and Editing: L.C. and M.C.; Funding acquisition: M.C.; Investigation: L.C. and S.V.; Methodology: M.C. and L.C.; Data curation: L.C. and S.V.; Formal analysis: L.C. and S.V.; Supervision: M.C.; Project administration: M.C. All authors have read and agreed to the published version of the manuscript.

Funding: This research received no external funding.

Data Availability Statement: The dataset is available upon request from the authors: The raw data supporting the conclusions of this article will be made available by the authors upon request.

Acknowledgments: The authors want to thank the Ministry of Fisheries, Marine Resources, and Agriculture of the Republic of Maldives for giving them the opportunity to carry out this study in the blue hole of Faanu Mudugau. We especially thank Albatros Top Boat and all the staff of the Duke of York boat for assistance during fieldwork, and the Colleagues of Save the Beach Maldives for helping us in all phases of the activity, from logistics to sampling. We also thank all the participants in the 2022 scientific expedition.

Conflicts of Interest: The authors declare no conflicts of interest. The funders had no role in the design of the study; in the collection, analyses, or interpretation of data; in the writing of the manuscript; or in the decision to publish the results.

References

1. Ahmed, F.; Fakhruddin, A.N.M. A Review on Environmental Contamination of Petroleum Hydrocarbons and its Biodegradation. *Int. J. Environ. Sci. Nat. Res.* **2018**, *11*, 63–69.
2. Hama Aziz, K.H.; Mustafa, F.S.; Omer, K.M.; Hama, S.; Hamarawf, R.F.; Rahman, K.O. Heavy metal pollution in the aquatic environment: Efficient and low-cost removal approaches to eliminate their toxicity: A review. *RSC Adv.* **2023**, *13*, 17595–17610. [[CrossRef](#)] [[PubMed](#)]
3. Brühl, C.A.; Engelhard, N.; Bakanov, N.; Wolfram, J.; Hertoge, K.; Zaller, J.G. Widespread contamination of soils and vegetation with current use pesticide residues along altitudinal gradients in a European Alpine valley. *Comm. Earth Environ.* **2024**, *5*, 72. [[CrossRef](#)]
4. Corcoran, J.; Winter, M.J.; Tyler, C.R. Pharmaceuticals in the aquatic environment: A critical review of the evidence for health effects in fish. *Critical Rev. Toxicol.* **2010**, *40*, 287–304. [[CrossRef](#)]
5. Harvey, P.J.; Taylor, M.P.; Handley, H.K. Widespread Environmental Contamination Hazards in Agricultural Soils from the Use of Lead Joints in Above Ground Large-Scale Water Supply Pipelines. *Water Air Soil Pollut.* **2015**, *226*, 178. [[CrossRef](#)]
6. Srivastava, R. Solid Waste Management and Its Impact on the Environment. In *Handbook of Research on Environmental and Human Health Impacts of Plastic Pollution*; Wani, K.A., Ariana, L., Zuber, S., Eds.; IGI Global: Hershey, PA, USA, 2020; pp. 389–400. [[CrossRef](#)]
7. Nriagu, J.O. A History of Global Metal Pollution. *Science* **1996**, *272*, 223–224. [[CrossRef](#)]

8. Khan, S.; Naushad, M.; Govarthan, M.; Iqbal, J.; Alfadul, S.M. Emerging contaminants of high concern for the environment: Current trends and future research. *Environ. Res.* **2022**, *207*, 112609. [[CrossRef](#)]
9. Sauv e, S.; Desrosiers, M. A review of what is an emerging contaminant. *Chem. Cent. J.* **2014**, *8*, 15. [[CrossRef](#)]
10. Diop, C.; Dewael e, D.; Diop, M.; Tour e, A.; Cabral, M.; Cazier, F.; Fall, M.; Diouf, A.; Ouddane, B. Assessment of contamination, distribution and chemical speciation of trace metals in water column in the Dakar coast and the Saint Louis estuary from Senegal, West Africa. *Mar. Pollut. Bull.* **2014**, *86*, 539–546. [[CrossRef](#)]
11. Manodori, L.; Gambaro, A.; Piazza, R.; Ferrari, S.; Stortini, A.M.; Moret, I.; Capodaglio, G. PCBs and PAHs in sea-surface microlayer and sub-surface water samples of the Venice Lagoon (Italy). *Mar. Pollut. Bull.* **2006**, *52*, 184–192. [[CrossRef](#)]
12. Stortini, A.M.; Martellini, T.; Del Bubba, M.; Lepri, L.; Capodaglio, G.; Cincinelli, A. n-Alkanes, PAHs and surfactants in the sea surface microlayer and sea water samples of the Gerlache Inlet Sea (Antarctica). *Microchem. J.* **2009**, *92*, 37–43. [[CrossRef](#)]
13. Nawrot, N.; Wojciechowska, E.; Mohsin, M.; Kuittinen, S.; Pappinen, A.; Rezanian, S. Trace Metal Contamination of Bottom Sediments: A Review of Assessment Measures and Geochemical Background Determination Methods. *Minerals* **2021**, *11*, 872. [[CrossRef](#)]
14. Soloveva, O.; Tikhonova, E.; Alyomov, S.; Mirzoeva, N.; Skuratovskaya, E.; Matishov, G.; Egorov, V. Distribution and Genesis of Aliphatic Hydrocarbons in Bottom Sediments of Coastal Water Areas of the Crimea (the Black and Azov Seas). *Water* **2024**, *16*, 2395. [[CrossRef](#)]
15. Al-Shamary, N.; Hassan, H.; Leit o, A.; Hutchinson, S.M.; Mondal, D.; Bayen, S. Baseline distribution of petroleum hydrocarbon contamination in the marine environment around the coastline of Qatar. *Mar. Pollut. Bull.* **2023**, *188*, 114655. [[CrossRef](#)]
16. Bosch, A.C.; O’Neill, B.; Sigge, G.O.; Kerwath, S.E.; Hoffman, L.C. Heavy metals in marine fish meat and consumer health: A review. *J. Sci. Food Agric.* **2016**, *96*, 32–48. [[CrossRef](#)]
17. Li, Y.; Chen, F.; Zhou, R.; Zheng, X.; Pan, K.; Qiu, G.; Wu, Z.; Chen, S.; Wang, D. A review of metal contamination in seagrasses with an emphasis on metal kinetics and detoxification. *J. Hazard. Mat.* **2023**, *454*, 131500. [[CrossRef](#)] [[PubMed](#)]
18. Gola, D.; Tyagi, P.K.; Arya, A.; Chauhan, N.; Agarwal, M.; Singh, S.K.; Gola, S. The impact of microplastics on marine environment: A review. *Environ. Nanotechnol. Monit. Manag.* **2021**, *16*, 100552. [[CrossRef](#)]
19. Sridharan, S.; Kumar, M.; Singh, L.; Bolan, N.S.; Saha, M. Microplastics as an emerging source of particulate air pollution: A critical review. *J. Hazard. Mat.* **2021**, *418*, 126245. [[CrossRef](#)]
20. Ya, H.; Jiang, B.; Xing, Y.; Zhang, T.; Lv, M.; Wang, X. Recent advances on ecological effects of microplastics on soil environment. *Sci. Total Environ.* **2021**, *798*, 149338. [[CrossRef](#)]
21. Bagaev, A.; Mizyuk, A.; Khatmullina, L.; Isachenko, I.; Chubarenko, I. Anthropogenic fibres in the Baltic Sea water column: Field data, laboratory and numerical testing of their motion. *Sci. Total Environ.* **2017**, *599–600*, 560–571. [[CrossRef](#)]
22. van Sebille, E.; Wilcox, C.; Lebreton, L.; Maximenko, N.; Hardesty, B.D.; van Franeker, J.A.; Eriksen, M.; Siegel, D.; Galgani, F.; Lavender Law, K. A global inventory of small floating plastic debris. *Environ. Res. Lett.* **2015**, *10*, 124006. [[CrossRef](#)]
23. Zhao, S.; Zettler, E.R.; Bos, R.P.; Lin, P.; Amaral-Zettler, L.A.; Mincer, T.J. Large quantities of small microplastics permeate the surface ocean to abyssal depths in the South Atlantic Gyre. *Glob. Change Biol.* **2022**, *28*, 2991–3006. [[CrossRef](#)]
24. Alomar, C.; Estarellas, F.; Deudero, S. Microplastics in the Mediterranean Sea: Deposition in coastal shallow sediments, spatial variation and preferential grain size. *Mar. Environ. Res.* **2016**, *115*, 1–10. [[CrossRef](#)] [[PubMed](#)]
25. De Ruijter, V.N.; Milou, A.; Costa, V. Assessment of microplastics distribution and stratification in the shallow marine sediments of Samos Island, Eastern Mediterranean Sea, Greece. *Med. Mar. Sci.* **2019**, *20*, 736–744. [[CrossRef](#)]
26. Abel, S.M.; Primpke, S.; Int-Veen, I.; Brandt, A.; Gerts, G. Systematic identification of microplastics in abyssal and hadal sediments of the Kuril Kamchatka trench. *Environ. Pollut.* **2021**, *269*, 116095. [[CrossRef](#)]
27. Cutroneo, L.; Capello, M.; Domi, A.; Consani, S.; Lamare, P.; Coyle, P.; Bertin, V.; Dornic, D.; Reboa, A.; Geneselli, I.; et al. Microplastics in the abyss: A first investigation into sediments at 2443-m depth (Toulon, France). *Environ. Sci. Pollut. Res.* **2022**, *29*, 9375–9385. [[CrossRef](#)]
28. Van Cauwenberghe, L.; Vanreusel, A.; Mees, J.; Janssen, C.R. Microplastic pollution in deep-sea sediments. *Environ. Pollut.* **2013**, *182*, 495–499. [[CrossRef](#)]
29. Pinheiro, L.M.; Ivar do Sul, J.A.; Costa, M.F. Uptake and ingestion are the main pathways for microplastics to enter marine benthos: A review. *Food Webs* **2020**, *24*, e00150. [[CrossRef](#)]
30. Sfriso, A.A.; Tomio, Y.; Rosso, B.; Gambaro, A.; Sfriso, A.; Corami, F.; Rastelli, E.; Corinaldesi, C.; Mistri, M.; Munari, C. Microplastic accumulation in benthic invertebrates in Terra Nova Bay (Ross Sea, Antarctica). *Environ. Int.* **2020**, *137*, 105587. [[CrossRef](#)]
31. Staffieri, E.; de Lucia, G.A.; Camedda, A.; Poeta, G.; Battisti, C. Pressure and impact of anthropogenic litter on marine and estuarine reptiles: An updated “blacklist” highlighting gaps of evidence. *Environ. Sci. Pollut. Res.* **2019**, *26*, 1238–1249. [[CrossRef](#)]
32. Wang, J.; Wang, M.; Ru, S.; Liu, X. High levels of microplastic pollution in the sediments and benthic organisms of the South Yellow Sea, China. *Sci. Tot. Environ.* **2019**, *651*, 1661–1669. [[CrossRef](#)] [[PubMed](#)]

33. Wootton, N.; Reis-Santos, P.; Gillanders, B.M. Microplastic in fish—A global synthesis. *Rev. Fish Biol. Fish.* **2021**, *31*, 753–771. [[CrossRef](#)]
34. Zantis, L.J.; Carroll, E.L.; Nelms, S.L.; Bosker, T. Marine mammals and microplastics: A systematic review and call for standardization. *Environ. Pollut.* **2021**, *269*, 116142. [[CrossRef](#)]
35. Chu, W.L.; Dang, N.L.; Kok, Y.Y.; Yap, K.S.I.; Phang, S.M.; Convey, P. Heavy metal pollution in Antarctica and its potential impacts on algae. *Polar Sci.* **2019**, *20*, 75–83. [[CrossRef](#)]
36. Darham, S.; Zakaria, N.N.; Zulkharnain, A.; Sabri, S.; Khalil, K.A.; Merican, F.; Gomez-Fuentes, C.; Lim, S.; Ahmad, S.A. Antarctic heavy metal pollution and remediation efforts: State of the art of research and scientific publications. *Braz. J. Microbiol.* **2023**, *54*, 2011–2026. [[CrossRef](#)]
37. Muir, D.C.G.; Wagemann, R.; Hargrave, B.T.; Thomas, D.J.; Peakall, D.B.; Norstrom, R.J. Arctic marine ecosystem contamination. *Sci. Total Environ.* **1992**, *122*, 75–134. [[CrossRef](#)] [[PubMed](#)]
38. Kothari, U.; Arnall, A. Contestation over an island imaginary landscape: The management and maintenance of touristic nature. *Environ. Plan. A* **2017**, *49*, 980–998. [[CrossRef](#)]
39. Zubair, S.; Bowen, D.; Elwin, J. Not quite paradise: Inadequacies of environmental impact assessment in the Maldives. *Tour. Manag.* **2011**, *32*, 225–234. [[CrossRef](#)]
40. U.S. Department of State. Report: 2024 Investment Climate Statements: Maldives. Available online: <https://www.state.gov/reports/2024-investment-climate-statements/maldives/> (accessed on 23 September 2024).
41. Ministry of Tourism, Government of Maldives. *Maldives Fifth Tourism Master Plan 2023–2027: Goals and Strategies*; Ministry of Tourism: Malé, Maldives. Available online: <https://www.tourism.gov.mv> (accessed on 23 September 2024).
42. Scheyvens, R. The challenge of sustainable tourism development in the Maldives: Understanding the social and political dimensions of sustainability. *Asia Pac. Viewp.* **2011**, *52*, 148–164. [[CrossRef](#)]
43. Aboobakur, S.; Samarakoon, M.B. Solid waste management in Kulhudhuffushi, Maldives; Most suitable solution for the Crisis. *Int. J. Environ. Agric. Biotechnol.* **2019**, *4*, 1853–1861. [[CrossRef](#)]
44. Wang, Y.; Ruiz-Aceved, A.; Rameez, E.; Raghavan, V.; Hussain, A.; Fei, X. Toward sustainable waste management in small islands developing states: Integrated waste-to-energy solutions in Maldives context. *Front. Environ. Sci. Eng.* **2024**, *18*, 24. [[CrossRef](#)]
45. Fallati, L.; Castiglioni, S.; Galli, P.; Riva, F.; Gracia-Lor, E.; Gonzalez-Marino, I.; Rousis, N.I.; Shifah, M.; Messa, M.C.; Strepparava, M.G.; et al. Use of legal and illegal substances in Malé (Republic of Maldives) assessed by wastewater analysis. *Sci. Tot. Environ.* **2020**, *698*, 134207.
46. Scott, P.J.B.; Davies, M. Retroactive determination of industrial contaminants in tropical marine communities. *Mar. Pollut. Bull.* **1997**, *34*, 975–980. [[CrossRef](#)]
47. Colombo, A.; Bettinetti, R.; Strona, G.; Cambria, F.; Fanelli, R.; Zubair, Z.; Galli, P. Maldives: An archipelago that burns. A first survey of PCDD/Fs and DL-PCBs from human activities. *Sci. Tot. Environ.* **2014**, *497–498*, 499–507. [[CrossRef](#)]
48. Rizzi, C.; Seveso, D.; Galli, P.; Villa, S. First record of emerging contaminants in sponges of an inhabited island in the Maldives. *Mar. Pollut. Bull.* **2020**, *156*, 111273. [[CrossRef](#)] [[PubMed](#)]
49. Nadhiya, A.; Khandaker, M.U.; Mahmud, S.; Abdullah, W.H. The presence of toxic heavy metals in tuna fishes from Laccadive Sea and concomitant health risk. *Radiat. Prot. Dosim.* **2023**, *199*, 2224–2228. [[CrossRef](#)]
50. Jumana, M.; Shaira, A. Baseline study to determine the presence of heavy metals in seawater of Thilafushi Island. *AIP Conf. Proc.* **2024**, *3245*, 060002. [[CrossRef](#)]
51. Imhof, H.K.; Sigl, R.; Brauer, E.; Feyl, S.; Giesemann, P.; Klink, S.; Leupolz, K.; Löder, M.G.; Löschel, L.A.; Missun, J.; et al. Spatial and temporal variation of macro-, meso- and microplastic abundance on a remote coral island of the Maldives, Indian Ocean. *Mar. Pollut. Bull.* **2017**, *116*, 340–347.
52. Patti, T.B.; Fobert, E.K.; Reeves, S.E.; Burke da Silva, K. Spatial distribution of microplastics around an inhabited coral island in the Maldives, Indian Ocean. *Sci. Tot. Environ.* **2020**, *748*, 141263.
53. Saliu, F.; Montano, S.; Garavaglia, M.G.; Lasagni, M.; Seveso, D.; Galli, P. Microplastic and charred microplastic in the Faafu Atoll, Maldives. *Mar. Pollut. Bull.* **2018**, *136*, 464–471. [[CrossRef](#)]
54. Raguso, C.; Saliu, F.; Lasagni, M.; Galli, P.; Clemenza, M.; Montano, S. First detection of microplastics in reef-building corals from a Maldivian atoll. *Mar. Pollut. Bull.* **2022**, *180*, 113773. [[CrossRef](#)] [[PubMed](#)]
55. Cutroneo, L.; Ahmed, H.; Azzola, A.; Fontana, H.; Geneselli, I.; Mancini, I.; Montefalcone, M.; Oprandi, A.; Pancrazi, I.; Vanin, S.; et al. First Chemical–Physical Measurements by Multi-Parameter Probe in the Blue Hole of Faanu Madugau (Ari Atoll, the Maldives). *Environments* **2023**, *10*, 180. [[CrossRef](#)]
56. Chen, B.; Yu, K.; Fu, L.; Wel, Y.; Liang, J.; Liao, Z.; Qin, Z.; Yu, X.; Deng, C.; Han, M.; et al. The diversity, community dynamics, and interactions of the microbiome in the world’s deepest blue hole: Insights into extreme environmental response patterns and tolerance of marine microorganisms. *Microbiol. Spectr.* **2023**, *11*, e00531-23. [[CrossRef](#)] [[PubMed](#)]
57. Li, Q.; Lei, Y.; Morard, R.; Li, T.; Wang, B. Diversity hotspot and unique community structure of foraminifera in the world’s deepest marine blue hole—Sansha Yongle Blue Hole. *Sci. Rep.* **2020**, *10*, 10257. [[CrossRef](#)] [[PubMed](#)]

58. Zhou, S.; Liu, J.; Yao, P.; Fu, L.; Yang, Z.; Zhang, Y.; Du, R.; Jia, C.; Chen, L.; Liang, J.; et al. Unique bacterial communities and lifestyles in deep ocean blue holes: Insights from the Yongle Blue Hole (South China Sea). *Front. Mar. Sci.* **2023**, *10*, 1086117. [[CrossRef](#)]
59. Wallace, E.; Donnelly, J.; van Hengstum, P.; Winkler, T.; Dizon, C.; LaBella, A.; Lopez, I.; d'Entremont, N.; Sullivan, R.; Woodruff, J.; et al. Regional shifts in paleohurricane activity over the last 1500 years derived from blue hole sediments offshore of Middle Caicos Island. *Quat. Sci. Rev.* **2021**, *268*, 107126. [[CrossRef](#)]
60. Schmitt, D.; Gischler, E.; Walkenfort, D. Holocene sediments of an inundated sinkhole: Facies analysis of the "Great Blue Hole", Lighthouse Reef, Belize. *Facies* **2021**, *67*, 10. [[CrossRef](#)]
61. Yu, X.; Duan, B.C.; Guo, K.; Li, T.; Feng, A.; Du, J.; Villemant, B.; Ning, Y.; Liu, Y. Mapping and U–Th dating of the world's deepest blue hole (South China Sea): Implications for its timing, possible volcanogenic origin, and Pleistocene eolianites in the Xisha Islands. *Mar. Geol.* **2022**, *447*, 106776. [[CrossRef](#)]
62. Colantoni, P.; Baldelli, G.; Bianchi, C.N.; Capaccioni, B.; Morri, C.; Sandrini, M.; Tassi, F. A cave flooded by marine water with hydrogen sulphide highlights the recent evolution of the Maldives (Indian Ocean): Preliminary notes. *Grotte D'Italia* **2003**, *4*, 29–37.
63. El-Haddad, K.; Fouad, M.; El-Sadeq, A.; El-Azim, I.A. Rapid Ecological Assessment of Coral Biodiversity and Reef Health in the Blue Hole Area, Dahab. In *Egypt's Protected Areas Self-Financing Project*; EPASP: Cairo, Egypt, 2018; Volume 71. [[CrossRef](#)]
64. Gischler, E.; Anselmetti, F.S.; Shinn, E.A. Seismic stratigraphy of the Blue Hole (Lighthouse Reef, Belize), a late Holocene climate and storm archive. *Mar. Geol.* **2013**, *344*, 155–162. [[CrossRef](#)]
65. Schmitt, D.; Gischler, E.; Birgel, D.; Peckmann, J.; Anselmetti, F.S.; Vogel, H. Great Blue Hole (Lighthouse Reef, Belize): A continuous, annually resolved record of Common Era Sea surface temperature, Atlantic Multidecadal Oscillation and cyclone-controlled run-off. *Quat. Sci. Rev.* **2020**, *247*, 106570. [[CrossRef](#)]
66. Zaini, N.; Briguglio, A.; Goeting, S.; Roslin, A.; Kocsis, L. Sedimentological characterisation of sea bottom samples collected offshore Muara and Tutong, Brunei Darussalam. *Bull. Geol. Soc. Malays.* **2020**, *70*, 139–151. [[CrossRef](#)]
67. Mogg, A.O.M.; Attard, K.M.; Stahl, H.; Brand, T.; Turnewitch, R.; Sayer, M.D.J. The influence of coring method on the preservation of sedimentary and biogeochemical features when sampling soft-bottom, shallow coastal environments. *Limnol. Oceanogr. Methods* **2017**, *15*, 905–915.
68. Rodríguez-Uribe, M.C.; Núñez-Cornú, F.J.; Chávez-Dagostino, R.M.; Trejo-Gómez, E. Granulometric Analysis of Shallow Vents Sediments at Banderas Bay (Mexico). *J. Mar. Sci. Eng.* **2020**, *8*, 342. [[CrossRef](#)]
69. Giraldo-Gómez, V.M.; Arena, L.; Capello, M.; Cutroneo, L.; Azzola, A.; Montefalcone, M.; Briguglio, A. Foraminifera and sediments cored from the bottom of the Faanu Mudugau Blue Hole, Ari Atoll, Maldives: Diversity, taphonomy and environmental reconstruction of an inhabitable substrate. *Mar. Geol.* **2024**, *478*, 107428.
70. Cutroneo, L.; Carbone, C.; Consani, S.; Vagge, G.; Canepa, G.; Capello, M. Environmental complexity of a port: Evidence from circulation of the water masses, and composition and contamination of bottom sediments. *Mar. Pollut. Bull.* **2017**, *119*, 184–194. [[CrossRef](#)] [[PubMed](#)]
71. Cutroneo, L.; Carbone, C.; Consani, S.; Capello, M. Sediment distribution on the continental shelf in relation to stream inputs and contamination: Hydrodynamic, chemical, mineralogical, and sedimentological characteristics (Ligurian Sea, Italy). *Environ. Sci. Pollut. Res.* **2020**, *27*, 43755–43768. [[CrossRef](#)]
72. Capello, M.; Cutroneo, L.; Consani, S.; Dinelli, E.; Vagge, G.; Carbone, C. Marine sediment contamination and dynamics at the mouth of a contaminated torrent: The case of the Gromolo Torrent (Sestri Levante, north-western Italy). *Mar. Pollut. Bull.* **2016**, *109*, 128–141. [[CrossRef](#)]
73. Cutroneo, L.; Reboa, A.; Geneselli, I.; Capello, M. Considerations on salts used for density separation in the extraction of microplastics from sediments. *Mar. Pollut. Bull.* **2021**, *166*, 112216. [[CrossRef](#)]
74. Pfeiffer, F.; Fischer, E.K. Various Digestion Protocols Within Microplastic Sample Processing—Evaluating the Resistance of Different Synthetic Polymers and the Efficiency of Biogenic Organic Matter Destruction. *Front. Environ. Sci.* **2020**, *8*, 572424. [[CrossRef](#)]
75. Reboa, A.; Cutroneo, L.; Consani, S.; Geneselli, I.; Petrillo, M.; Besio, G.; Capello, M. Mugilidae fish as bioindicator for monitoring plastic pollution: Comparison between a commercial port and a fishpond (north-western Mediterranean Sea). *Mar. Pollut. Bull.* **2022**, *177*, 113531. [[CrossRef](#)] [[PubMed](#)]
76. Xu, J.L.; Thomas, K.V.; Luo, Z.; Gowen, A.A. FTIR and Raman imaging for microplastics analysis: State of the art, challenges and prospects. *TrAC Trends Anal. Chem.* **2019**, *119*, 115629. [[CrossRef](#)]
77. Adikaram, M.; Pitawala, A.; Ishiga, H.; Jayawardana, D.; Eichler, C.M. An Ecological Risk Assessment of Sediments in a Developing Environment—Batticaloa Lagoon, Sri Lanka. *J. Mar. Sci. Eng.* **2021**, *9*, 73. [[CrossRef](#)]
78. Liu, D.; Wang, J.; Yu, H.; Gao, H.; Xu, W. Evaluating ecological risks and tracking potential factors influencing heavy metals in sediments in an urban river. *Environ. Sci. Eur.* **2021**, *33*, 42. [[CrossRef](#)]

79. Oksanen, J.; Blanchet, F.G.; Friendly, M.; Kindt, R.; Legendre, P.; McGlenn, D.; Minchin, P.R.; O'hara, R.B.; Simpson, G.L.; Solymos, P.; et al. *Vegan: Community Ecology Package*. R Package Version 2.5-4. 2019. Available online: <https://CRAN.R-project.org/package=vegan> (accessed on 28 February 2025).
80. Shepard, F.P. Nomenclature based on sand-silt-clay ratios. *J. Sediment. Petrol.* **1954**, *24*, 151–158.
81. Gischler, E. Sedimentation on Rasdhoo and Ari Atolls, Maldives, Indian Ocean. *Facies* **2006**, *52*, 341–360.
82. Morgan, K.M.; Kench, P.S. A detrital sediment budget of a Maldivian reef platform. *Geomorphology* **2014**, *222*, 122–131. [[CrossRef](#)]
83. Rasheed, S.; Warder, S.C.; Plancherel, Y.; Piggott, M.D. Response of tidal flow regime and sediment transport in North Malé Atoll, Maldives, to coastal modification and sea level rise. *Ocean Sci.* **2021**, *17*, 319–334. [[CrossRef](#)]
84. Wadey, M.; Brown, S.; Nicholls, R.J.; Haigh, I. Coastal flooding in the Maldives: An assessment of historic events and their implications. *Nat. Hazards* **2017**, *89*, 131–159.
85. Gischler, E.; Shinn, E.A.; Oschmann, W.; Fiebig, J.; Buster, N.A. A 1500-year Holocene Caribbean climate archive from the Blue Hole, Lighthouse Reef, Belize. *J. Coast. Res.* **2008**, *24*, 1495–1505.
86. Lüdmann, T.; Betzler, C.; Lindhorst, S. The Maldives, a key location of carbonate drifts. *Mar. Geol.* **2022**, *450*, 106838.
87. Kench, P.S.; Brander, R.W.; Parnell, K.E.; McLean, R.F. Wave energy gradients across a Maldivian atoll: Implications for island geomorphology. *Geomorphology* **2006**, *81*, 1–17. [[CrossRef](#)]
88. Secrieru, D.; Oaie, G. The relation between the grain size composition of the sediments from the NW Black Sea and their total organic carbon (TOC) content. *Geo-Eco-Mar.* **2009**, *15*, 5–11.
89. Chester, R.; Jickells, T. *Marine Geochemistry*, 3rd ed.; Wiley-Blackwell A John Wiley & Sons, Ltd.: Hoboken, NJ, USA, 2012; pp. 11–30.
90. Prince, K.; Laya, J.C.; Budd, D.; Manche, C.J.; Jacquemyn, C. Dolomite occurrence within drift deposits, Maldives archipelago. *Sediment. Geol.* **2024**, *470*, 106711.
91. Alonso-Garcia, M.; Reolid, J.; Jimenez-Espejo, F.J.; Bialik, O.M.; Zarikina, C.A.A.; Laya, J.C.; Carrasquiera, I.; Reijmer, J.J.G.; Eberli, G.P.; Betzler, C. Sea-level and monsoonal control on the Maldives carbonate platform (Indian Ocean) over the last 1.3 million years. *Clim. Past* **2024**, *20*, 547–571. [[CrossRef](#)]
92. Ausili, A.; Berducci, M.T.; Maggi, C.; Sesta, G. *Analisi di Sostanze Prioritarie in Matrici Marine. Parte, I. Verifica delle Metodologie Ufficiali Esistenti e loro Applicabilità alle Matrici Marine*; ISPRA—Manuali e Linee Guida 175/2018; ISPRA: Rome, Italy, 2018; p. 45. Available online: https://www.isprambiente.gov.it/files2018/pubblicazioni/manuali-linee-guida/MLG_175_18.pdf (accessed on 10 February 2025).
93. Canadian Council of Ministers of the Environment. Canadian Sediment Quality Guidelines for the Protection of Aquatic Life: Mercury. In *Canadian Environmental Quality Guidelines*; Canadian Council of Ministers of the Environment: Winnipeg, MB, Canada, 1999. Available online: <https://www.ccme.ca/en/res/mercury-canadian-sediment-quality-guidelines-for-the-protection-of-aquatic-life-en.pdf> (accessed on 2 December 2024).
94. Republic of Maldives. Minimata Initial Assessment Report 2019. Available online: <https://www.environment.gov.mv/v2/wp-content/files/publications/20200315-pub-minamata-initial-assessment-report-2019.pdf> (accessed on 2 December 2024).
95. Sharifuzzaman, S.M.; Rahman, H.; Ashekuzzaman, S.M.; Islam, M.M.; Chowdhury, S.R.; Hossain, M.S. Heavy Metals Accumulation in Coastal Sediments. In *Environmental Remediation Technologies for Metal-Contaminated Soils*; Hasegawa, H., Rahman, I., Rahman, M., Eds.; Springer: Tokyo, Japan, 2016. [[CrossRef](#)]
96. Sidhu, G.P.S.; Bali, A.S. Chapter 11—Cd in the environment: Uptake, toxicity and management. In *Appraisal of Metal(loids) in the Ecosystem*; Kumar, V., Sharma, A., Setia, R., Eds.; Elsevier: Amsterdam, The Netherlands, 2022; pp. 283–300. [[CrossRef](#)]
97. Mikhailenko, A.V.; Ruban, D.A.; Ermolaev, V.A.; van Loon, A.J. Cadmium Pollution in the Tourism Environment: A Literature Review. *Geosciences* **2020**, *10*, 242. [[CrossRef](#)]
98. El-Sorogy, A.S.; Youssef, M.; Al-Kahtany, K.; Al-Otaiby, N. Assessment of arsenic in coastal sediments, seawaters and molluscs in the Tarut Island, Arabian Gulf, Saudi Arabia. *J. Afr. Earth Sci.* **2016**, *113*, 65–72. [[CrossRef](#)]
99. Steibl, S.; Franke, J.; Laforsch, C. Tourism and urban development as drivers for invertebrate diversity loss on tropical islands. *R. Soc. Open Sci.* **2021**, *8*, 210411. [[CrossRef](#)]
100. Dong, M.; Zhang, Q.; Xing, X.; Chen, W.; She, Z.; Luo, Z. Raman spectra and surface changes of microplastics weathered under natural environments. *Sci. Tot. Environ.* **2020**, *739*, 139990.
101. Liu, Y.; Hu, J.; Lin, L.; Yang, B.; Huang, M.; Chang, M.; Huang, X.; Dai, Z.; Sun, S.; Ren, L.; et al. Overcoming the fluorescent interference during Raman spectroscopy detection of microplastics. *Sci. Tot. Environ.* **2023**, *897*, 165333.
102. Dabrowska, A. Raman Spectroscopy of Marine Microplastics—A short comprehensive compendium for the environmental scientists. *Mar. Environ. Res.* **2021**, *168*, 105313. [[CrossRef](#)] [[PubMed](#)]
103. Song, Y.K.; Hong, S.H.; Eo, S.; Shim, W.J. A comparison of spectroscopic analysis methods for microplastics: Manual, semi-automated, and automated Fourier transform infrared and Raman techniques. *Mar. Pollut. Bull.* **2021**, *173*, 113101. [[CrossRef](#)]
104. Cabernard, L.; Roscher, L.; Lorenz, C.; Gerdtts, G.; Primpke, S. Comparison of Raman and Fourier Transform Infrared Spectroscopy for the Quantification of Microplastics in the Aquatic Environment. *Environ. Sci. Technol.* **2018**, *52*, 13279–13288. [[CrossRef](#)] [[PubMed](#)]

105. Albarano, L.; Maggio, C.; La Marca, A.; Iovine, R.; Lofrano, G.; Guida, M.; Vaiano, V.; Carotenuto, M.; Pedatella, S.; Spica, V.R.; et al. Risk assessment of natural and synthetic fibers in aquatic environment: A critical review. *Sci. Tot. Environ.* **2024**, *934*, 173398. [[CrossRef](#)] [[PubMed](#)]
106. Li, Y.; Zhang, H.; Tang, C. A review of possible pathways of marine microplastics transport in the ocean. *Anthr. Coasts* **2020**, *3*, 6–13. [[CrossRef](#)]
107. Tatsii, D.; Bucci, S.; Bhowmick, T.; Guettler, J.; Bakels, L.; Bagheri, G.; Stohl, A. Shape Matters: Long-Range Transport of Microplastic Fibers in the Atmosphere. *Environ. Sci. Technol.* **2024**, *58*, 671–682. [[CrossRef](#)]

Disclaimer/Publisher’s Note: The statements, opinions and data contained in all publications are solely those of the individual author(s) and contributor(s) and not of MDPI and/or the editor(s). MDPI and/or the editor(s) disclaim responsibility for any injury to people or property resulting from any ideas, methods, instructions or products referred to in the content.